Article

Electroactive Supramolecular Self-Assembled Fibers Comprised of Doped Tetrathiafulvalene-Based Gelators

Tetsu Kitamura, Suguru Nakaso, Norihiro Mizoshita, Yusuke Tochigi, Takeshi Shimomura, Masaya Moriyama, Kohzo Ito, and Takashi Kato

J. Am. Chem. Soc., **2005**, 127 (42), 14769-14775• DOI: 10.1021/ja053496z • Publication Date (Web): 30 September 2005

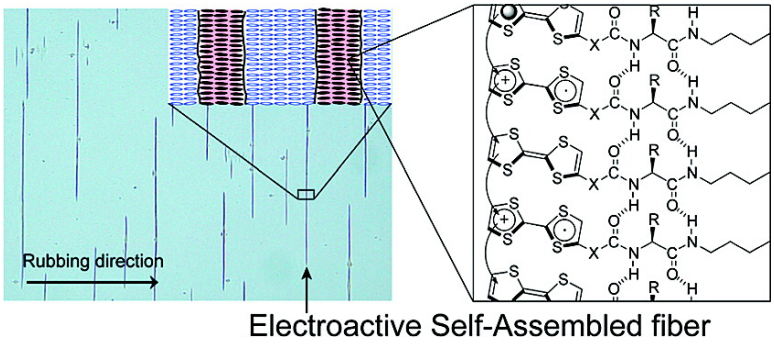

More About This Article

Additional resources and features associated with this article are available within the HTML version:

- Supporting Information
- Links to the 24 articles that cite this article, as of the time of this article download
- Access to high resolution figures
- Links to articles and content related to this article
- Copyright permission to reproduce figures and/or text from this article

View the Full Text HTML

J|A|C|S
ARTICLES
Published on Web 09/30/2005

Electroactive Supramolecular Self-Assembled Fibers Comprised of Doped Tetrathiafulvalene-Based Gelators

Tetsu Kitamura,[†] Suguru Nakaso,[†] Norihiro Mizoshita,[†] Yusuke Tochigi,[†] Takeshi Shimomura,[‡] Masaya Moriyama,[†] Kohzo Ito,[‡] and Takashi Kato*[,†]

Contribution from the Department of Chemistry and Biotechnology, School of Engineering, The University of Tokyo, Hongo, Bunkyo-ku, Tokyo 113-8656, Japan, and Graduate School of Frontier Sciences, The University of Tokyo, Kashiwanoha, Kashiwa-shi, Chiba 277-8561, Japan

Received May 28, 2005; Revised Manuscript Received August 23, 2005; E-mail: kato@chiral.t.u-tokyo.ac.jp

Abstract: New electroactive supramolecular fibers have been formed by self-assembly of the derivatives of tetrathiafulvalene (TTF) in liquid crystals. These derivatives are designed and prepared by introducing the TTF moiety to the scaffold derived from amino acids such as L-isoleucine whose derivatives function as organogelators. These TTF-based gelators form stable fibrous aggregates in liquid crystals. These fibers are the first example of hydrogen-bonded one-dimensional aggregates having electroactive moieties whose electrical conductivities were measured after doping. Their electronic states have also been characterized by spectroscopic methods. Unidirectionally aligned fibers are formed in the oriented liquid crystal solvents on the rubbed polyimide surface for further functionalization of the fibers.

Introduction

Supramolecular self-assembly is one of the promising approaches for the fabrication of molecular materials.[1] For example, molecular self-assembly from solution states often leads to the formation of one-dimensional (1D) solid fibers.[2] This process has attracted attention because 1D fibrous solids, ranging from the submicrometer to nanometer scale, are easily obtained by simple self-assembly through noncovalent interactions such as hydrogen bonding, ionic interactions, and $\pi-\pi$ stacking in a variety of solvents.[2] The network formation of the fibers in the solvents leads to the preparation of physical gels. The molecules that drive physical gelation are called gelators.[2] If functional moieties are introduced into each component of the gelators, new functional 1D objects would be obtained. Our new approach is to obtain electroactive 1D fibers through molecular self-assembly processes of gelators having tetrathiafulvalene (TTF) moieties. Intensive studies have focused on TTF for the preparation of conductive materials in bulk[3] and thin film states.[4] High conductivities can be expected for TTF-based materials through the formation of charge-transfer (CT) complexes with electron acceptors such as tetracyano-*p*-quinodimethane (TCNQ) and iodine.[3] Molecular switches incorporating TTF moieties have also been prepared.[5]

For self-assembled fibers incorporating the TTF moieties, two examples of bis-arborol-TTF[6] and tetra(TTF-crown-ether) phthalocyanine[7] were prepared. However, no conductivities of these solid fibers were measured. Some examples of self-assembled electroactive fibers based on other electroactive moieties were obtained by using oligothiophene,[8] aromatic disks,[9] phthalocyanine,[10] and oligo(*p*-phenylenevinylene).[11]

[†] School of Engineering.
[‡] Graduate School of Frontier Sciences.

(1) (a) Service, R. F. *Science* **2002**, *295*, 2398−2399. (b) Lehn, J.-M. *Science* **2002**, *295*, 2400−2403. (c) Kato, T. *Science* **2002**, *295*, 2414−2418. (d) Hoeben, F. J. M.; Jonkheijm, P.; Meijer, E. W.; Schenning, A. P. H. J. *Chem. Rev.* **2005**, *105*, 1491−1546. (e) Hartgerink, J. D.; Zubarev, E. R.; Stupp, S. I. *Curr. Opin. Solid State Mater. Sci.* **2001**, *5*, 355−361. (f) Ikkala, O.; ten Brinke, G. *Chem. Commun.* **2004**, 2131−2137. (g) Simpson, C. D.; Wu, J.; Watson, M. D.; Müllen, K. *J. Mater. Chem.* **2004**, *14*, 494−504. (h) Bushey, M. L.; Hwang, A.; Stephens, P. W.; Nuckolls, C. *Angew. Chem., Int. Ed.* **2002**, *41*, 2828−2831. (i) Yoshio, M.; Mukai, T.; Ohno, H.; Kato, T. *J. Am. Chem. Soc.* **2004**, *126*, 994−995. (j) Sawamura, M.; Kawai, K.; Matsuo, Y.; Kanie, K.; Kato, T.; Nakamura, E. *Nature* **2002**, *419*, 702−705. (k) van Herrikhuyzen, J.; Syamakumari, A.; Schenning, A. P. H. J.; Meijer, E. W. *J. Am. Chem. Soc.* **2004**, *126*, 10021−10027. (l) Smith, R. C.; Fischer, W. M.; Gin, D. L. *J. Am. Chem. Soc.* **1997**, *119*, 4092−4093.

(2) (a) Abdallah, D. J.; Weiss, R. G. *Adv. Mater.* **2000**, *12*, 1237−1247. (b) van Esch, J. H.; Feringa, B. L. *Angew. Chem., Int. Ed.* **2000**, *39*, 2263−2266. (c) Meléndez, R. E.; Carr, A. J.; Linton, B. R.; Hamilton, A. D. *Struct. Bonding* **2000**, *96*, 31−61. (d) *Molecular Gels*; Weiss, R. G., Terech, P., Eds.; Kluwer Academic Press: Amsterdam, 2005. (e) Sugiyasu, K.; Fujita, N.; Shinkai, S. *J. Synth. Org. Chem. Jpn.* **2005**, *63*, 359−369. (f) Shinkai, S.; Murata, K. *J. Mater. Chem.* **1998**, *8*, 485−495.

(3) (a) Bryce, M. R. *Chem. Soc. Rev.* **1991**, *20*, 355−390. (b) Nielsen, M. B.; Lomholt, C.; Becher, J. *Chem. Soc. Rev.* **2000**, *29*, 153−164. (c) Bryce, M. R. *J. Mater. Chem.* **2000**, *10*, 589−598. (d) Segura, J. L.; Martín, N. *Angew. Chem., Int. Ed.* **2001**, *40*, 1372−1409. (e) Schukat, G.; Fanghänel, E. *Sulfur Rep.* **2003**, *24*, 1−190. (f) Wu, P.; Saito, G.; Imaeda, K.; Shi, Z.; Mori, T.; Enoki, T.; Inokuchi, H. *Chem. Lett.* **1986**, 441−444. (g) Kobayashi, A.; Fujiwara, E.; Kobayashi, H. *Chem. Rev.* **2004**, *104*, 5243−5264.

(4) (a) Dhindsa, A. S.; Bryce, M. R.; Lloyd, J. P.; Petty, M. C. *Synth. Met.* **1988**, *27*, B563−B568. (b) Richard, J.; Vandevyver, M.; Barraud, A.; Morand, J. P.; Lapouyade, R.; Delhaes, P.; Jacquinot, J. F.; Roulliay, M. *J. Chem. Soc., Chem. Commun.* **1988**, 754−756. (c) Dhindsa, A. S.; Song, Y.-P.; Badyal, J. P.; Bryce, M. R.; Lvov, Y. M.; Petty, M. C.; Yarwood, J. *Chem. Mater.* **1992**, *4*, 724−728. (d) Bryce, M. R.; Petty, M. C. *Nature* **1995**, *374*, 771−776. (e) Bryce, M. R.; Moore, A. J.; Batsanov, A. S.; Howard, J. A. K.; Petty, M. C.; Williams, G.; Rotello, V.; Cuello, A. *J. Mater. Chem.* **1999**, *9*, 2973−2978. (f) Akutagawa, T.; Kakiuchi, K.; Hasegawa, T.; Nakamura, T.; Christensen, C. A.; Becher, J. *Langmuir* **2004**, *20*, 4187−4195.

(5) (a) Collier, C. P.; Mattersteig, G.; Wong, E. W.; Luo, Y.; Beverly, K.; Sampaio, J.; Raymo, F. M.; Stoddart, J. F.; Heath, J. R. *Science* **2000**, *289*, 1172−1175. (b) Stoddart, J. F.; et al. *Chem.-Eur. J.* **2003**, *9*, 2982−3007. (c) Liu, Y.; Flood, A. H.; Moskowitz, R. M.; Stoddart, J. F. *Chem.-Eur. J.* **2005**, *11*, 369−385.

(6) Jørgensen, M.; Bechgaard, K.; Bjørnholm, T.; Sommer-Larsen, P.; Hansen, L. G.; Schaumburg, K. *J. Org. Chem.* **1994**, *59*, 5877−5882.

(7) Sly, J.; Kasák, P.; Gomar-Nadal, E.; Rovira, C.; Górriz, L.; Thordarson, P.; Amabilino, D. B.; Rowan, A. E.; Nolte, R. J. M. *Chem. Commun.* **2005**, 1255−1257.

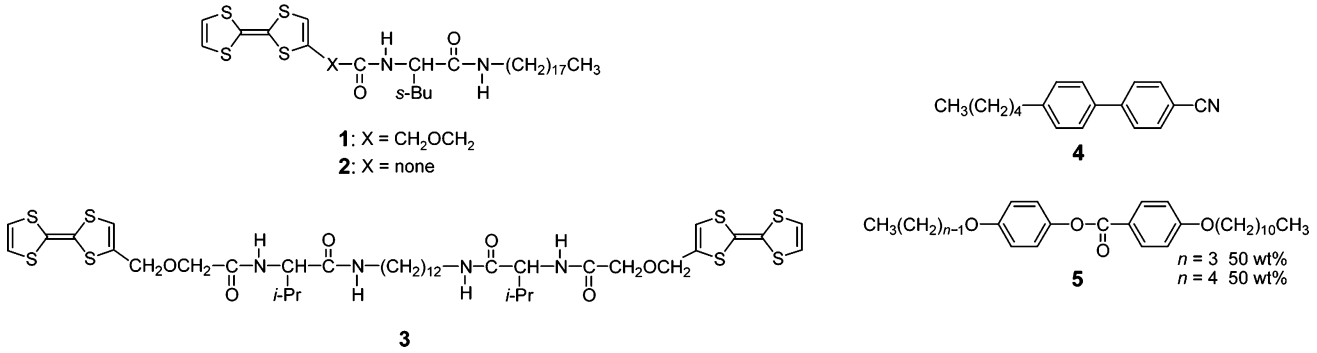

Figure 1. Molecular structures of hydrogen bonding TTF derivatives **1**−**3** and liquid crystals **4** and **5**.

Here, we report on new electroactive self-assembled fibers consisting of organogelators based on TTF. We have found that stable fibrous aggregates are formed in aromatic liquid crystals. Iodine-doping has been successfully carried out for the solid-state self-assembled fibers, leading to the formation of 1D CT complexes. The conductivities of these 1D materials have been measured with platinum electrodes (1 mm in width) on a silicon wafer. Moreover, we have obtained aligned electroactive fibers for their further functionalization.

Results and Discussion

Molecular Design and Syntheses of TTF Derivatives as Self-Assembled Materials. TTF derivatives **1**−**3** containing amino acid moieties have been prepared in this study (Figure 1). They are designed to form hydrogen-bonded fibrous aggregates. For compound **1**, the L-isoleucine-based scaffold is connected to the TTF moiety through a $-CH_2OCH_2-$ linker, while the TTF moiety is directly attached to the scaffold for compound **2**. Simpler amino acid derivatives such as L-isoleucine were found to form fibrous aggregates in common organic solvents[12,13] and in liquid crystals.[14] For compound **3**, a $-CH_2OCH_2-$ linker is introduced to both sides of the dimeric L-valine scaffold, which can also form fibrous aggregates in common organic solvents.[13] Compounds **1**−**3** were synthesized by condensation of TTF-based carboxylic acids and L-isoleucylaminooctadecane or 1,12-bis(L-valylamino)dodecane.

Fibrous Self-Assembly of 1−3 in Common Organic Solvents. Compounds **1**−**3** do not show excellent gelling ability for common organic solvents, although simpler amino acid derivatives were reported to act as efficient gelators.[12,13] For example, compound **1** gelates only toluene and ethyl acetate below 10 °C, while no gelation by **1** is observed for polar solvents such as acetone, ethanol, methanol, and DMF. No stable fibrous aggregates of **1**−**3** are obtained in these common organic solvents. Such lower gelling abilities have been caused by the introduction of the bulky π-conjugated moieties.

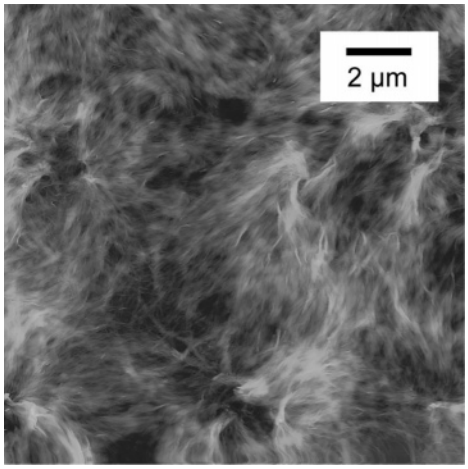

Figure 2. AFM image of fibrous aggregates of **1** formed in **4**.

Fibrous Self-Assembly of 1−3 in Liquid Crystals. We have found that in aromatic liquid crystals of **4** and **5** (Figure 1), stable fibrous aggregates of **1** and **3** are formed and these anisotropic solvents are gelated efficiently by these compounds. A biphenyl compound (**4**) shows a nematic phase below 34 °C. Phenyl benzoate liquid crystal **5**, which is the 50:50 (wt %) mixture of 4-propoxyphenyl 4-undecyloxybenzoate and 4-butoxyphenyl 4-undecyloxybenzoate, exhibits a nematic phase between 83 and 78 °C and a smectic A phase below 78 °C. The introduction of π-conjugated moiety to the gelators may enhance their gelling ability for those aromatic liquid crystals.[15] Such behavior was observed for gelators containing cyanobiphenyl[15a] and azobenzene[15b] moieties.

Compounds **1** and **3** form fibrous aggregates of 20−50 nm in diameter in liquid crystals **4** and **5** at room temperature (Figure 2) (see Supporting Information), although no stable fibers of **1**−**3** are obtained in common organic solvents. Compound **2** forms aggregates only below room temperature. Figure 3a shows the phase transition behavior of the mixtures of **1** and **4** (**1**/**4**). The mixtures of **1**/**4** containing more than 4

(8) (a) Schoonbeek, F. S.; van Esch, J. H.; Wegewijs, B.; Rep, D. B. A.; de Haas, M. P.; Klapwijk, T. M.; Kellogg, R. M.; Feringa, B. L. *Angew. Chem., Int. Ed.* **1999**, *38*, 1393−1397. (b) Meijer, E. W.; et al. *J. Am. Chem. Soc.* **2002**, *124*, 1269−1275. (c) Messmore, B. W.; Hulvat, J. F.; Sone, E. D.; Stupp, S. I. *J. Am. Chem. Soc.* **2004**, *126*, 14452−14458.
(9) Hill, J. P.; Jin, W.; Kosaka, A.; Fukushima, T.; Ichihara, H.; Shimomura, T.; Ito, K.; Hashizume, T.; Ishii, N.; Aida, T. *Science* **2004**, *304*, 1481−1483.
(10) (a) van Nostrum, C. F.; Picken, S. J.; Schouten, A.-J.; Nolte, R. J. M. *J. Am. Chem. Soc.* **1995**, *117*, 9957−9965. (b) Engelkamp, H.; Middelbeek, S.; Nolte, R. J. M. *Science* **1999**, *284*, 785−788.
(11) (a) Ajayaghosh, A.; George, S. J. *J. Am. Chem. Soc.* **2001**, *123*, 5148−5149. (b) Jonkheijm, P.; Hoeben, F. J. M.; Kleppinger, R.; van Herrikhuyzen, J.; Schenning, A. P. H. J.; Meijer, E. W. *J. Am. Chem. Soc.* **2003**, *125*, 15941−15949.
(12) Hanabusa, K.; Hiratsuka, K.; Kimura, M.; Shirai, H. *Chem. Mater.* **1999**, *11*, 649−655.
(13) Hanabusa, K.; Tanaka, R.; Suzuki, M.; Kimura, M.; Shirai, H. *Adv. Mater.* **1997**, *9*, 1095−1097.
(14) (a) Mizoshita, N.; Kutsuna, T.; Hanabusa, K.; Kato, T. *Chem. Commun.* **1999**, 781−782. (b) Kato, T.; Kutsuna, T.; Yabuuchi, K.; Mizoshita, N. *Langmuir* **2002**, *18*, 7086−7088. (c) Suzuki, Y.; Mizoshita, N.; Hanabusa, K.; Kato, T. *J. Mater. Chem.* **2003**, *13*, 2870−2874. (d) Mizoshita, N.; Hanabusa, K.; Kato, T. *Adv. Funct. Mater.* **2003**, *13*, 313−317. (e) Mizoshita, N.; Suzuki, Y.; Hanabusa, K.; Kato, T. *Adv. Mater.* **2005**, *17*, 692−696.
(15) (a) Kato, T.; Kondo, G.; Hanabusa, K. *Chem. Lett.* **1998**, 193−194. (b) Moriyama, M.; Mizoshita, N.; Yokota, T.; Kishimoto, K.; Kato, T. *Adv. Mater.* **2003**, *15*, 1335−1338.

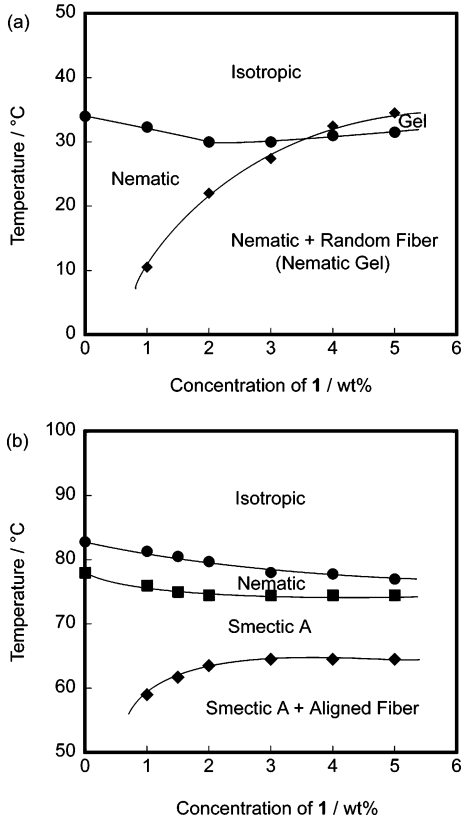

Figure 3. Phase transition behavior of the mixtures of (a) **1**/**4** and (b) **1**/**5**.

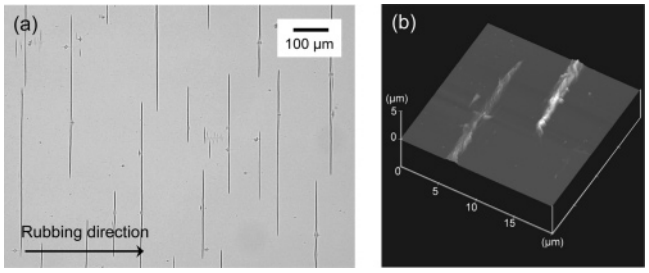

Figure 4. (a) Optical photomicrograph and (b) AFM image of fibrous aggregates of **1** formed in the oriented smectic A phase of **5**.

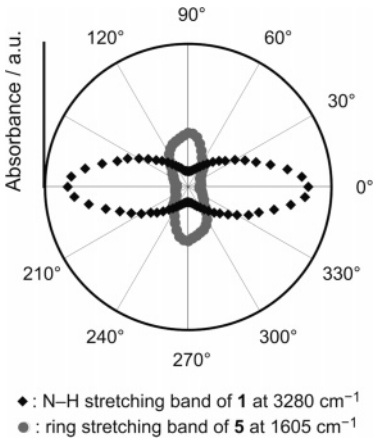

Figure 5. Polar plot of the absorbance of the IR bands for the mixture of **1**/**5** (2 wt %) at 60 °C in the parallel rubbed cell.

wt % of **1** show sol−gel transition temperatures higher than the isotropic−nematic transition temperatures. Compound **1** forms randomly dispersed fibers in the isotropic phase of **4**.

For the mixtures of **1**/**4** containing less than 3 wt % of **1**, fibrous aggregation of **1** occurs at temperatures lower than isotropic−nematic transition temperatures. So, we expected that oriented fibers of **1** were formed in the oriented monodomain of the nematic phases on the rubbed polyimide surface. We previously reported that simpler amino acid derivatives formed well-oriented fibers in the homogeneously oriented nematic phases.[14c−e] However, in contrast, no alignment of self-assembled fibers of **1** is observed. Randomly dispersed fibers of **1** are formed even in the oriented nematic state of **4** on the rubbed polyimide surface. Such observation shows that molecular structures of the gelators are important for an efficient template effect in the liquid crystals and compound **1** is not suitable for the formation of aligned fibers in the nematic phase.

In the homogeneously oriented smectic A phase of **5**, aligned fibrous aggregates of **1** grow along the smectic layers (Figure 4). This observation shows that **5** functions as a template for the alignment of the fibers of **1**. Figure 3b shows the phase transition behavior of the mixtures of **1**/**5**. Fibrous aggregates of **1** are formed in the smectic A phase on cooling the mixtures of **1**/**5** from the isotropic states. The lengths and distances of aligned fibers depend on the concentration of **1** and the cooling rate. We have obtained the fibrous aggregates of **1** with a length of more than 500 μm in **5** by slow cooling. For the mixtures of **3**/**5**, no fibers are formed in the temperature range of the smectic phase of **5** because of the higher aggregation temperatures of **3**.

Characterization of Fibrous Aggregates. Thermal properties of the fibers depend on the chemical structures of **1**−**3**. Compounds **1** and **3** form thermally more stable fibers than does **2**. For example, fibrous aggregations of **1**−**3** (3 wt %) in **4** occur at 27 °C for **1**, at 8 °C for **2**, and at 33 °C for **3**, respectively. These results suggest that the introduction of a $-CH_2OCH_2-$ spacer between the TTF and the amino acid moieties is effective to induce stable 1D molecular assemblies. To understand these differences, we have examined the hydrogen-bonded states of the amino acid moieties by IR measurements. In the isotropic states of the mixtures of **1**/**4**, **2**/**4**, and **3**/**4** at 120 °C, the N−H and C═O stretching bands of the amide groups are observed at 3400 (br) and 1678 cm^{-1}, respectively. These bands show that the amide groups are free from hydrogen bonding. For the fibrous aggregates of both **1** and **3** formed in **4** at room temperature, the N−H and C═O stretching bands are observed at 3280 and 1638 cm^{-1}, respectively. The amide bands of the fibers of **2** appear at 3299 and 1651 cm^{-1}. These observations indicate that compounds **1** and **3** form intermolecular hydrogen bonds in the parallel β-sheet conformation,[16] while compound **2** forms in a random conformation. These IR results show that the hydrogen bonding can be more stable for **1** and **3** due to the presence of the spacer. Without the spacer, the stacking of the TTF moiety directly disturbs the formation of the stable conformation for the hydrogen-bonded amide group.

Polarized IR spectra for the oriented mixtures of **1**/**5** show that the N−H stretching band of **1** at 3280 cm^{-1} is perpendicular to the ring stretching band of **5** at 1605 cm^{-1} (Figure 5). This result indicates that the hydrogen-bonded chains formed by TTF derivative **1** align along the fiber direction. A schematic

(16) Toniolo, C.; Palumbo, M. *Biopolymers* **1977**, *16*, 219−224.

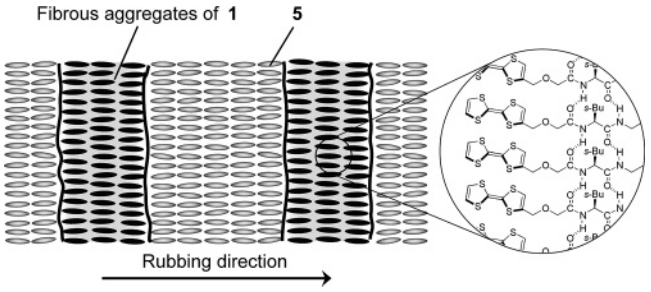

Figure 6. Schematic illustration of the oriented hierarchical structure of the mixture of **1**/**5** in the parallel rubbed cell.

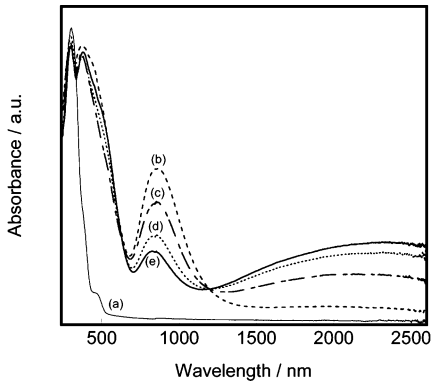

Figure 7. UV−vis−NIR spectra for the fibrous aggregates of **1** before and after iodine-doping for 2 min: (a) before doping, (b) immediately after doping, (c) 5 h after doping, (d) 1 day after doping, and (e) 1 week after doping.

illustration of the anisotropic hierarchical structure consisting of the TTF derivative and liquid crystal materials is shown in Figure 6.

UV−vis spectra for **1**−**3** were measured in the solution (in chloroform: 1×10^{-5} mol L^{-1}) and in the aggregated fibrous solid states (xerogels obtained from the gels based on **4**) (see Supporting Information). Blue shifts (318 to 300 nm for **1**, 318 to 306 nm for **2**, and 314 to 296 nm for **3**) of the $\pi-\pi^*$ transition peak for the TTF ring are observed in the aggregation of **1**−**3**, which is attributable to exciton coupling of TTF rings due to the formation of H aggregates.[17] Such blue shifts were previously observed for fibrous aggregates containing oligothiophene groups.[8]

Doping of Electroactive Self-Assembled Fibers with Electron Acceptors. We have succeeded in iodine-doping for the self-assembled fibers maintaining the assembled solid structures. Electronic states and assembled structures before and after iodine-doping were examined by UV−vis−NIR (Figure 7) and IR (Figure 8) spectroscopic methods. Xerogels obtained from **4** were used for the measurements. Figure 7a presents the UV−vis−NIR spectrum for the fibrous aggregates of **1** before doping. Immediately after exposure to iodine vapor for 2 min in a sealed container, new absorption bands are observed at 380, 500 (shoulder), and 850 nm (Figure 7b). The appearance of the band at 850 nm suggests the formation of a full CT state as illustrated in Figure 9a.[18] The bands at 380 and 500 nm are attributed to intramolecular transitions of the TTF cation radical. When the

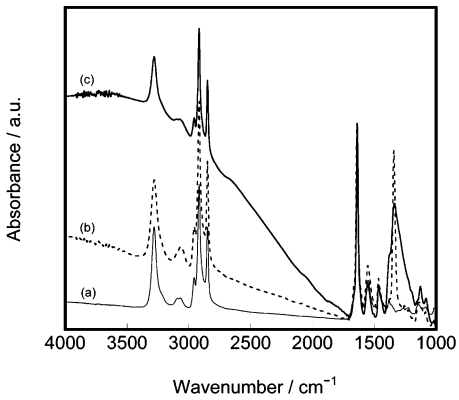

Figure 8. IR spectra for the fibrous aggregates of **1** before and after iodine-doping for 2 min: (a) before doping, (b) immediately after doping, and (c) 1 week after doping.

sample is kept in air for 5 h after exposure to iodine vapor, the spectrum of the sample significantly changes as follows. The CT band at 850 nm becomes weaker in intensity, and a broad band arises at 2300 nm (Figure 7c). This broad band is ascribed to a band due to a partial CT (mixed-valence) state (Figure 9b).[18] The spectrum reaches the steady state after 1 week. No significant change is then observed for a few months. These results are in good agreement with the previous results on iodine-doped Langmuir−Blodgett films having TTF moieties.[4] These films were first oxidized to a full (1:1) CT state (TTF^+I^- or $TTF^+I_3^-$) by exposure to iodine vapor. The full CT state changed to a more stable mixed-valence conducting state ($(TTF)I_x$ or $(TTF)(I_3)_x$ ($x < 1$)) with gradual release of iodine over time.

The UV−vis−NIR spectra of compound **3** before and after iodine-doping are similar to those of compound **1** (see Supporting Information). The CT band is observed at 1800 nm, which suggests the formation of a mixed-valence state, and its energy gap of the fibers of **3** is larger than that of **1**. The TTF moieties of **1** may be fixed in a more favorable conformation for electronic conduction in the fibers than those of **3**.

The changes in the IR spectra also show the formation of the CT complex (Figure 8). A broad CT band of the mixed-valence state extends over the IR region (~1700 cm^{-1}). In addition, upon doping a new sharp band appears at 1342 cm^{-1}, which is due to the coupling of a conduction electron with the vibrational mode of the TTF moiety called electron-molecular vibration (e-mv) coupling (Figure 8b).[19] This band becomes broader with the formation of a mixed-valence state (Figure 8c). For the aligned fibrous aggregates of **1** formed in the oriented smectic A phase of **5**, an anisotropic feature is observed in the CT band (Figure 10). This result suggests that electronic conduction may occur along the aligned fibers of **1**. The N−H and C═O stretching bands of the amide groups do not shift after iodine-doping, which shows that the doping does not change the hydrogen-bonded structure. We also measured X-ray diffraction patterns for the iodine-doped samples. The peak due to the distance of TTF stacking is 4.1 Å before and after doping, indicating that molecular assembled structures are not disturbed by iodine-doping (see Supporting Information).[20]

We have obtained UV−vis−NIR and IR spectra for TCNQ-doped fibrous aggregates of **1** (see Supporting Information). In

(17) Kasha, M.; Rawls, H. R.; El-Bayoumi, M. A. *Pure Appl. Chem.* **1965**, *11*, 371−392.
(18) (a) Sugano, T.; Yakushi, K.; Kuroda, H. *Bull. Chem. Soc. Jpn.* **1978**, *51*, 1041−1046. (b) Torrance, J. B.; Scott, B. A.; Welber, B.; Kaufman, F. B.; Seiden, P. E. *Phys. Rev. B* **1979**, *19*, 730−741.
(19) Bozio, R.; Zanon, I.; Girlando, A.; Pecile, C. *J. Chem. Phys.* **1979**, *71*, 2282−2293.

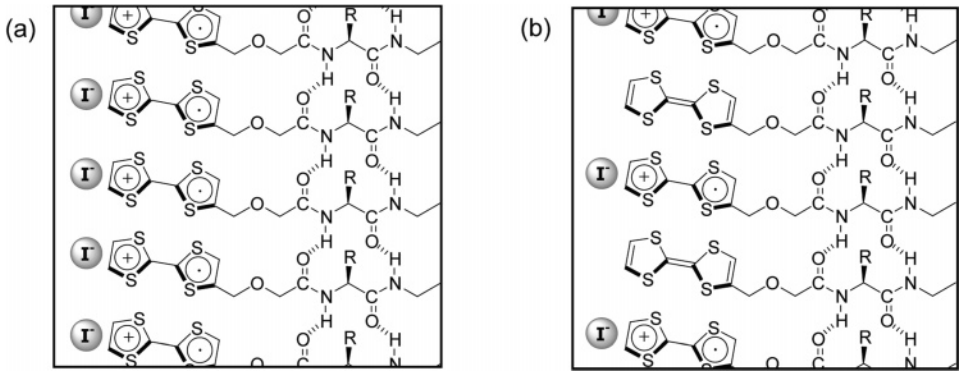

Figure 9. Schematic illustration of aggregates of hydrogen bonding TTF derivatives doped with iodine: (a) a full charge-transfer state, and (b) a partial charge-transfer (mixed-valence) state.

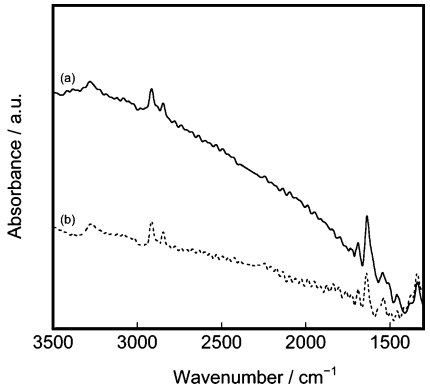

Figure 10. Polarized IR spectra for aligned fibrous aggregates of **1**, 1 week after iodine-doping for 2 min: (a) parallel to the fiber direction, and (b) perpendicular to the fiber direction.

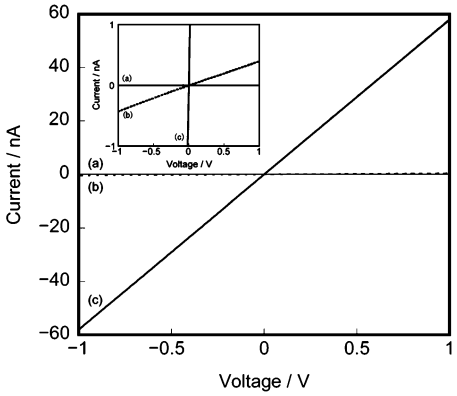

Figure 11. Current−voltage characteristics for fibrous aggregates of **1** before and after iodine-doping for 2 min: (a) before doping, (b) immediately after doping, and (c) 1 week after doping.

these spectra, the CT band indicative of the formation of a mixed-valence state is observed at 3500 cm^{-1}. The band due to the e-mv coupling between conduction electron and the TTF moiety is observed at 1300 cm^{-1}. The IR spectrum of the fibrous aggregates of **1** also shows that its hydrogen-bonded structure does not change after doping with TCNQ. A stable mixed-valence state is formed immediately after doping with TCNQ, while 1 week is needed to form the stable state for the iodine-doping.

Measurements of the Electrical Conductivities of the Fibers. The electrical conductivities of randomly dispersed fibrous aggregates of the TTF derivatives (xerogels obtained from the gels based on **4**) were measured at room temperature in vacuo using a two-probe technique (Figure 11). The fibers of **1** in the neutral state before doping behave as insulator ($\sigma_{rt} < 3 \times 10^{-10}$ S cm^{-1}), whereas the conductivity increases immediately after iodine-doping for 2 min ($\sigma_{rt} = 2 \times 10^{-7}$ S cm^{-1}). The UV−vis−NIR and IR spectra of the doped sample suggest that iodine-doping leads to the formation of the full CT state. One week after exposure to iodine vapor, the conductivity reaches a maximum at 3×10^{-5} S cm^{-1} (see Supporting Information). The spectra indicate that the mixed valence state is formed. The current−voltage characteristics of fibrous aggregates show an ohmic behavior between −1 and +1 V (Figure 11). The contact resistance should be sufficiently small because we see no threshold voltages in the $I-V$ curves of the samples that correspond to energies required for injecting hole carriers into the fibers.[9] The conductivity of the fibrous aggregates of **3** also increases until it reaches a value of $10^{-5}-10^{-6}$ S cm^{-1}. The fibers of **1** doped with TCNQ show a conductivity of 1×10^{-5} S cm^{-1}. These results suggest that the fibers forming the CT states function as conductive materials.

We examined temperature dependence of the conductivities of the fibrous aggregates of **1**. Ten days after being iodine-doped, the sample was used for the measurements. The conductivity exhibits an exponential dependence on temperature, which is expressed as $\sigma = \sigma_0 \exp(-E_a/k_BT)$ (Figure 12). This behavior is characteristic of a semiconductor. The thermal activation energy for the conductivity in the range 290−190 K is estimated to be 0.35 eV. For self-assembled materials relevant to the fibrous materials reported here, Langmuir−Blodgett (LB) films containing TTF moieties, the conductivities were between 10^{-1} and 10^{-3} S cm^{-1},[4] which were higher than those of the present system (10^{-5} S cm^{-1}). The thermal activation energies for the LB films were 0.10−0.25 eV,[4] which are lower than those of the present fibrous materials (0.35 eV). In the present materials for the measurements of the fibrous materials, the single fibers have not yet bridged the electrodes. In this case, the conduction process between fibers is incorporated into the conductivities.

Conclusion

We have succeeded in the fabrication of electroactive self-assembled fibers. The formation of hydrogen bonding between

(20) We have found that iodine-doping for the TTF derivatives in the fibers induces thermal stabilization of the aggregates. For example, doping 0.25 equiv of iodine into the mixtures of **1**/**4** (3 wt %) raises fiber formation temperatures by 15 °C (see Supporting Information). Partial oxidization of the TTF moieties of **1** by iodine enhances stacking of the TTF moieties, which leads to the formation of thermally more stable fibers.

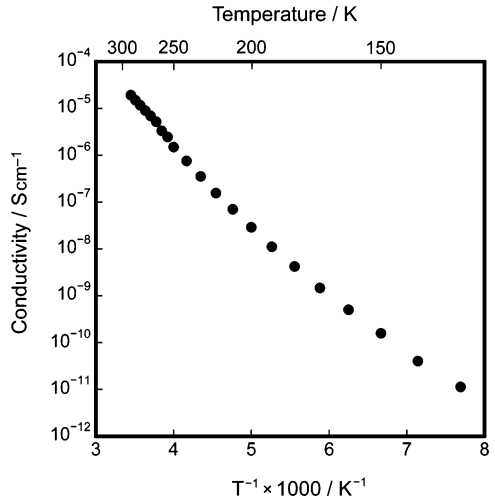

Figure 12. Temperature dependence of the conductivities of fibrous aggregates of **1**, 10 days after iodine-doping for 2 min.

amino acid derivatives having TTF moieties in liquid crystals has led to the formation of the electroactive fibrous aggregates. The doping of fibers by iodine results in the formation of charge transfer states exhibiting semiconducting values of about 10^{-5} S cm^{-1}. This may lead to the fabrication of self-assembled 1D solid conductive fibers, of which direction of orientation is controlled on the substrate.

Experimental Section

General. ^{1}H and ^{13}C NMR spectra were recorded on a JEOL GX-270 or a JEOL JNM-LA400 spectrometer with use of TMS as the internal standard. IR measurements were conducted on a Jasco FT/IR-660 Plus spectrometer. UV−vis−NIR absorption spectra were recorded on a Agilent 8453 or a Hitachi U-4000 spectrometer. Elemental analyses were carried out with a Perkin-Elmer 2400II elemental analyzer. Mass spectra (MALDI-TOF-MS) were recorded on a Biosystems BioSpectrometry Workstation model Voyager-DE STR spectrometer using dithranol as the matrix. Recycling preparative GPC was carried out with a Japan Analytical Industry LC-908 chromatograph. Phase transition behavior of the materials was examined by differential scanning calorimetry (DSC) using a Mettler DSC 30 or a Netzsch DSC 204. The heating and cooling rates were 5 °C min^{-1}. Transition temperatures were taken at the maximum of the transition peaks on cooling. A polarizing optical microscope Olympus BX51 equipped with a Mettler FP82HT hot stage was used for visual observation. Tapping-mode atomic force microscope (AFM) observation was performed with a Digital Instruments Nanoscope IIIa equipped with a cantilever (NCH-10V) at room temperature in air. X-ray diffraction measurements were carried out on a Rigaku RINT 2500 diffractometer using Ni-filtered Cu Kα radiation.

Materials. All chemical reagents and solvents were obtained from commercial sources and used without further purification. As for tetrahydrofuran (THF) and *N*,*N*-dimethylformamide (DMF), commercially available anhydrous solvents were used. All synthetic reactions were carried out under an argon atmosphere. Nematic liquid crystal, 4-cyano-4′-pentylbiphenyl (**4**), was purchased from Tokyo Kasei Kogyo. Liquid crystal components of **5**, 4-propoxyphenyl 4-undecyloxybenzoate and 4-butoxyphenyl 4-undecyloxybenzoate, were synthesized by dehydration condensation of corresponding 4-alkyloxyphenols and 4-alkyloxybenzoic acids. Compound **4** shows an isotropic−nematic transition at 34 °C. Compound **5** shows isotropic−nematic and nematic−smectic A transitions at 83 and 78 °C, respectively.

Synthesis of Ethyl (4-Tetrathiafulvalenylmethoxy)acetate. A mixture of 2-(hydroxymethyl)tetrathiafulvalene (0.81 g, 3.4 mmol),[21] NaH (0.27 g, 11 mmol), and dry THF (100 mL) was stirred for 1 h. Then ethyl bromoacetate (2.0 g, 12 mmol) was added, and the reaction mixture was stirred for 12 h at room temperature. The reaction mixture was dissolved in chloroform and washed with water. The organic phase was dried with $MgSO_4$, and the solvent was evaporated. The crude material was purified by column chromatography, using an eluent of hexane/chloroform (1:1). Yield: 0.45 g (41%). ^{1}H NMR (270 MHz, $CDCl_3$): δ 6.31 (s, 2H), 6.26 (s, 1H), 4.38 (s, 2H), 4.23 (q, J = 7.3 Hz, 2H), 4.10 (s, 2H), 1.30 ppm (t, J = 7.1 Hz, 3H). ^{13}C NMR (100 MHz, $CDCl_3$): δ 169.8, 133.3, 119.1, 118.9, 117.7, 68.0, 66.6, 61.1, 14.2 ppm. IR (KBr): ν 2925, 2854, 1748, 1211, 1125, 1094, 795, 778, 646 cm^{-1}. MS (MALDI-TOF): calcd, 319.97 (M^+); found, 320.10 (M^+).

Synthesis of (4-Tetrathiafulvalenylmethoxy)acetic Acid. A mixture of ethyl (2-tetrathiafulvalenylmethoxy)acetate (0.45 g, 1.4 mmol), KOH (0.85 g, 15 mmol), ethanol (27 mL), and water (10 mL) was refluxed for 1 h. The reaction mixture was acidified with 5% hydrochloric acid, dissolved in chloroform, and washed with water. The organic phase was dried with $MgSO_4$, and the solvent was evaporated. Yield: 0.37 g (90%). ^{1}H NMR (270 MHz, $CDCl_3$): δ 6.32 (s, 2H), 6.29 (s, 1H), 4.40 (s, 2H), 4.16 ppm (s, 2H). ^{13}C NMR (100 MHz, $CDCl_3$): δ 173.7, 132.7, 119.0, 118.3, 108.9, 68.1, 66.0 ppm. IR (KBr): ν 2923, 2853, 1734, 1203, 1120, 795, 648 cm^{-1}. MS (MALDI-TOF): calcd, 291.94 (M^+); found, 292.08 (M^+).

Synthesis of *N*-[(4-Tetrathiafulvalenylmethoxy)acetyl]-L-isoleucylaminooctadecane (1). A mixture of (2-tetrathiafulvalenylmethoxy)-acetic acid (0.36 g, 1.2 mmol), L-isoleucylaminooctadecane (0.70 g, 1.8 mmol), 1-ethyl-3-(3-dimethylaminopropyl)carbodiimide hydrochloride (EDC, 0.47 g, 2.5 mmol), 4-(*N*,*N*-dimethylamino)pyridine (DMAP, 0.015 g, 0.12 mmol), and dry THF (50 mL) was stirred at room temperature for 1 day. The reaction mixture was dissolved in chloroform and washed with saturated NH_4Cl aq, saturated $NaHCO_3$ aq, and saturated NaCl aq. The organic phase was dried with $MgSO_4$, and the solvent was evaporated. The crude material was purified by column chromatography, using an eluent of chloroform. The product was reprecipitated with hexane from chloroform. Yield: 0.38 g (47%). mp 134 °C. ^{1}H NMR (270 MHz, $CDCl_3$): δ 6.96 (d, J = 8.9 Hz, 1H), 6.31 (s, 2H), 6.29 (s, 1H), 5.79 (t, J = 4.2 Hz, 1H), 4.38−4.25 (m, 2H), 4.19 (dd, J = 8.7, 7.7 Hz, 1H), 4.05−3.95 (m, 2H), 3.34−3.18 (m, 2H), 2.01−1.92 (m, 1H), 1.52−1.09 (m, 34H), 0.98−0.85 ppm (m, 9H). ^{13}C NMR (100 MHz, $CDCl_3$): δ 170.6, 169.0, 134.9, 119.0, 112.0, 68.8, 57.4, 39.6, 37.0, 32.0, 29.5, 26.9, 25.0, 22.7, 15.6, 14.2, 11.3 ppm. UV ($CHCl_3$): λ 318, 370 (sh), 445 nm (sh). IR (KBr): ν 3280, 3060, 2958, 2919, 2850, 1644, 1550, 796, 778, 645 cm^{-1}. Anal. Calcd for $C_{33}H_{56}N_2O_3S_4$ (657.07): C, 60.32; H, 8.59; N, 4.26. Found: C, 60.34; H, 8.59; N, 4.53. MS (MALDI-TOF): calcd, 656.32 (M^+); found, 656.34 (M^+).

Synthesis of *N*-(4-Tetrathiafulvalenylcarbonyl)-L-isoleucylaminooctadecane (2). A mixture of 2-carboxytetrathiafulvalene (0.13 g, 0.54 mmol),[21] L-isoleucylaminooctadecane (0.21 g, 0.54 mmol), EDC (0.15 g, 0.80 mmol), DMAP (0.0070 g, 0.0057 mmol), and dry THF (15 mL) was stirred at room temperature for 1 day. The reaction mixture was dissolved in chloroform and washed with saturated NH_4Cl aq, saturated $NaHCO_3$ aq, and saturated NaCl aq. The organic phase was dried with $MgSO_4$, and the solvent was evaporated. The crude material was purified by column chromatography, using an eluent of hexane/ethyl acetate (3:1). The product was recrystallized from methanol. Yield: 0.12 g (36%). mp 68 °C. ^{1}H NMR (270 MHz, $CDCl_3$): δ 7.11 (s, 1H), 6.48 (d, J = 8.6 Hz, 1H), 6.32 (s, 2H), 5.94 (t, J = 4.2 Hz, 1H), 4.23 (dd, J = 8.3, 7.9 Hz, 1H), 3.35−3.15 (m, 2H), 1.94−1.81 (m, 1H), 1.56−1.07 (m, 34H), 0.94−0.85 ppm (m, 9H). ^{13}C NMR (100

(21) (a) Green, D. C. *J. Org. Chem.* **1979**, *44*, 1476−1479. (b) Garín, J.; Orduna, J.; Uriel, S.; Moore, A. J.; Bryce, M. R.; Wegener, S.; Yufit, D. S.; Howard, J. A. K. *Synthesis* **1994**, 489−493.

MHz, $CDCl_3$): δ 163.2, 159.1, 130.7, 126.6, 58.7, 39.8, 32.5, 29.6, 26.8, 25.3, 23.0, 15.4, 14.0, 11.1 ppm. UV ($CHCl_3$): λ 318, 420, 600 nm. IR (KBr): ν 3293, 3068, 2954, 2914, 2847, 1650, 1545, 795, 775, 644, 633 cm^{-1}. Anal. Calcd for $C_{31}H_{52}N_2O_2S_4$ (613.02): C, 60.74; H, 8.55; N, 4.57. Found: C, 60.15; H, 8.80; N, 4.64. MS (MALDI-TOF): calcd, 612.29 (M^+); found, 612.34 (M^+).

Synthesis of 1,12-Bis[*N*-{(2-tetrathiafulvalenylmethoxy)acetyl}-L-valylamino]dodecane (3). A mixture of (2-tetrathiafulvalenylmethoxy)acetic acid (0.31 g, 1.1 mmol), 1,12-bis(L-valylamino)-dodecane (0.19 g, 0.47 mmol), EDC (0.40 g, 2.1 mmol), DMAP (0.014 g, 0.11 mmol), and dry THF (30 mL) was stirred at room temperature for 2 days. The reaction mixture was dissolved in chloroform and washed with saturated NH_4Cl aq and water. The organic phase was dried with $MgSO_4$, and the solvent was evaporated. The crude material was purified by column chromatography, using an eluent of chloroform/methanol (20:1). The product was recrystallized from ethyl acetate/methanol (10:1), followed by GPC. Yield: 0.24 g (54%). mp 110 °C. ^1H NMR (400 MHz, $CDCl_3$): δ 7.05 (d, J = 9.2 Hz, 2H), 6.32 (s, 4H), 6.29 (s, 2H), 6.25 (t, J = 5.8 Hz, 2H), 4.38−4.27 (m, 4H), 4.22 (dd, J = 7.2, 7.2 Hz, 2H), 4.05−3.94 (m, 4H), 3.33−3.15 (m, 4H), 2.20−2.11 (m, 2H), 1.51−1.24 (m, 20H), 0.98−0.95 ppm (m, 12H). ^{13}C NMR (100 MHz, $CDCl_3$): δ 170.5, 169.0, 132.8, 119.1, 119.0, 118.2, 112.1, 68.7, 68.2, 58.3, 39.5, 30.8, 29.4, 29.3, 29.1, 26.8, 19.3, 18.3 ppm. UV ($CHCl_3$): λ 314, 370 (sh), 450 nm (sh). IR (KBr): ν 3291, 3063, 2958, 2924, 2851, 1646, 1523, 795, 776, 638 cm^{-1}. Anal. Calcd for $C_{40}H_{58}N_4O_6S_8$ (947.44): C, 50.71; H, 6.17; N, 5.91. Found: C, 50.63; H, 6.17; N, 5.95. MS (MALDI-TOF): calcd, 946.21 (M^+); found, 946.27 (M^+) (see Supporting Information).

Gelation Test. In a typical gelation experiment, an organic solvent (0.1 mL) was added to a weighed sample (4 mg) in a test tube. The tube was sealed and heated until a clear solution was obtained. The resultant solution was allowed to cool to room temperature, and gelation was checked visually. When the tube could be inverted without any flow, it was considered to be a gel. If the mixture remained as a solution at room temperature, it was further cooled in a refrigerator (−20 °C), and if gelation occurred at lower temperatures, it was also considered to be a gel.

Preparation of Liquid Crystal Composites. The composites were prepared by mixing liquid crystals and hydrogen bonding TTF derivatives in test tubes. The mixtures in the sealed test tubes were heated to isotropic states, and then cooled to the required temperatures. For homogeneously aligned states, the liquid crystal mixtures in the isotropic states were filled in glass sandwich cells (thickness: 5 μm) coated with polyimide layers (JSR AL1254), whereby the rubbing direction of the two surfaces was parallel. The mixtures in the cells were cooled from the isotropic states at required rates, which were controlled with a Mettler FP82HT hot stage. For polarized IR measurements, sample cells were prepared by sandwiching the mixtures between two CaF_2 plates coated with polyimide (JSR AL1254), whereby the rubbing direction of the two surfaces was parallel.

Preparation of Xerogel for Characterization. AFM observations, UV−vis−NIR and IR spectroscopies, X-ray diffraction, and electrical conductivity measurements were performed for xerogels obtained from the mixtures of **4** or **5** and hydrogen-bonding TTF derivatives. The xerogels were prepared by immersing the liquid crystal mixtures in hexane for a few hours to remove the liquid crystalline component and were finally dried at room temperature.

Doping of Self-Assembled Fibers with Electron Acceptor. Iodine-doping of the fibrous aggregates of hydrogen-bonding TTF derivatives was carried out by exposure to iodine vapor in a sealed container. To examine the dependence of fiber formation temperatures of hydrogen-bonding TTF derivatives on molar ratio of iodine, a given amount of iodine was added to the liquid crystal mixture. Doping of the fibrous aggregates with tetracyano-*p*-quinodimethane (TCNQ) was carried out by placing one drop of acetonitrile solution of TCNQ (0.5 g L^{-1}) on the sample. After 1 min, the droplet was blown with air, and then the fibers were washed with acetonitrile.

Electrical Conductivity Measurements. The measurements of electrical conductivities were carried out using a standard two-probe method in vacuo ($<10^{-5}$ Torr) with a source measurement unit (Keithley 236). The platinum electrodes (1 mm in width) used in the measurements were situated on a silicon wafer coated with an insulating SiO_2 layer (150 nm), which were placed 100 μm apart. The conductivity values were calculated for the volume of the fibrous aggregates of hydrogen-bonding TTF derivatives, which bridge electrodes (see Supporting Information).

Acknowledgment. Financial support of a Grant-in-Aid for Creative Scientific Research of "Invention of Conjugated Electronic Structures and Novel Functions" (No. 16GS0209) (T.K.) from the Japan Society for the Promotion of Science (JSPS) and for The 21st Century COE Program of "The Frontier of Fundamental Chemistry Focusing on Molecular Dynamism" (T.K.) from the Ministry of Education, Culture, Sports, Science and Technology is gratefully acknowledged. We thank Mr. Hideki Ichihara and Ms. Aoi Inomata for their assistance in the measurements of conductivities. We are also grateful to JSR Corp. for supplying the polyimide material.

Supporting Information Available: Synthetic scheme of **1**−**3**, phase transition diagrams for **3**/**4** and **3**/**5**, UV−vis absorption spectra of **1**, UV−vis−NIR and IR spectra for the fibrous aggregates of **3**, plot of the fiber formation temperature of **4**/**1**, X-ray diffraction patterns, UV−vis−NIR and IR spectra for the fibrous aggregates of **1** doped with TCNQ, conductivity change with time after iodine-doping, an illustration of the setup for conductivity measurements, and complete refs 5b and 8b. This material is available free of charge via the Internet at http://pubs.acs.org.

JA053496Z